11th International Conference on Vibration Problems
Z. Dimitrovová *et.al.* (eds.)
Lisbon, Portugal, 9–12 September 2013

ACTIVE VIBRATION ISOLATION VIA DECOMPOSITION OF TRAVELING WAVES

Edwin Kreuzer[1], Ludwig Krumm[1], Marc-André Pick[1], Eugen Solowjow*[1], Michael Steidl[2]

[1]Hamburg University of Technology, Germany
{kreuzer, pick, ludwig.krumm, eugen.solowjow}@tuhh.de

[2]Hasse & Wrede GmbH, Germany
michael.steidl@hassewrede.de

Keywords: Axial vibrations, active vibration isolation, model-free control, decomposition of traveling waves.

Abstract. *The need for isolating structures from surrounding vibrations arises frequently in many engineering applications. Examples include the isolation of manufacturing operations against seismic inputs as well as the development of suspension systems in automotive applications. We present a model-free active control method for the vibration isolation of a rigid item that is elastically mounted to a slender rod which is subject to axial vibrations. A controlled linear actuator is placed between the rod and the item. It allows the displacement of the item in relation to the rod, with the goal of reducing the vibration transmissibility from rod to item. The key idea for controller development is to consider the axial vibrations as a superposition of mechanical waves traveling in opposite directions inside the rod. The actuator is then controlled in order to reflect the waves that are traveling towards the item, thus interrupting the energy propagation path between rod and item. We demonstrate that the algorithm developed by Kreuzer and Steidl [1] can be used for the decomposition of axial vibrations into traveling waves. The only required sensor inputs are the time-varying axial displacements of two arbitrary points on the rod. The control algorithm is implemented for a numerical example and results show that the concept works very effectively. Furthermore, we show with an experimental setup the feasibility of the delicate measurements that provide the required axial displacements of the rod.*

1 INTRODUCTION

In many contexts, ranging from automotive applications to manufacturing, it is desired to isolate an elastically mounted item from a vibrating structure. The concept of vibration isolation can be illustrated with the single degree-of-freedom system shown in Fig. 1a [2]. The system consists of a rigid item that is supported by an isolator which is connected to a foundation. A displacement $\overline{u}$ is imposed on the foundation and causes a displacement u_m of the item. The goal of vibration isolation is to design an isolator in order to minimize the motion transmissibility from the foundation to the rigid item.

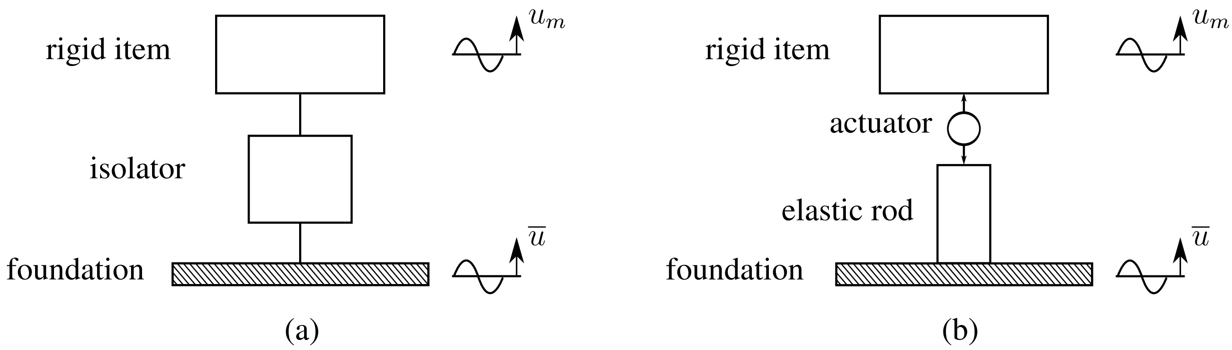

Figure 1: Schematic diagrams of a vibration isolation system. Motion $\overline{u}$ is imposed at the foundation and motion u_m is transmitted to the rigid item: (a) A general system; (b) A system for active vibration isolation with wave effects in the elastic rod.

Various methods for vibration isolation and, therefore, for isolator design exist. They can be grouped in passive [2, 3], semi-active [4, 5], and active isolators [6, 7]. In general, the categorization follows from the requirement of external energy supply and the possibility for control. Both, passive and semi-active isolators have system immanent drawbacks due to the uncontrollability of the resilient forces. Active isolators overcome these disadvantages by applying external energy to the system by means of actuators. Most control algorithms applied in active vibration isolation do not consider the distributed mass of isolator elements, mainly because it introduces undesired wave effects. In the present paper, we demonstrate an active isolator that exploits these wave effects.

The considered class of mechanical systems is shown schematically in Fig. 1b. It consists of a rigid item that is mounted to an elastic rod which is subject to foundation excitation. A linear actuator is placed between the rod and the item and allows the displacement of the item in relation to the rod. Foundation excitation results in axial displacements of the rod, which can be regarded as a superposition of two waves traveling in opposite directions. A fast actuator can reflect the waves traveling towards the rigid item, and thus isolate the item from foundation excitations. However, this strategy requires exact knowledge of the waves traveling towards the item. Since it is in general not possible to measure these waves directly, we use a version of the algorithm presented in [1]. It allows the exact decomposition of axial displacements into traveling waves and is based on the finite traveling speed of mechanical waves. The only inputs required are displacement measurements of two arbitrary rod points. Unlike traditional active vibration isolation concepts, our approach does not require a sophisticated system model. In fact, the only necessary system parameter is the speed of sound of the rod material. Numerical simulations show that the presented concept performs very effectively. An experimental setup demonstrates the feasibility of the required displacement measurements.

The remainder of this paper is organized as follows. In Section 2, we present a detailed system model, yet without the actuator. In Section 3, the derivation of the control concept that is based on the decomposition of traveling waves is performed. In Section 4, we apply the control algorithm to the model and present a numerical example. Finally, in Section 5 we show the feasibility of the displacement measurements in our experimental setup.

2 DYNAMICAL SYSTEM

Consider a rigid item of mass m attached via a spring to an elastic, isotropic and homogenous rod which is subject to vibrations, see Fig. 2. The system can be described within the framework of linear elastodynamics [8]. Thereby, uniaxial stress and strain are assumed.

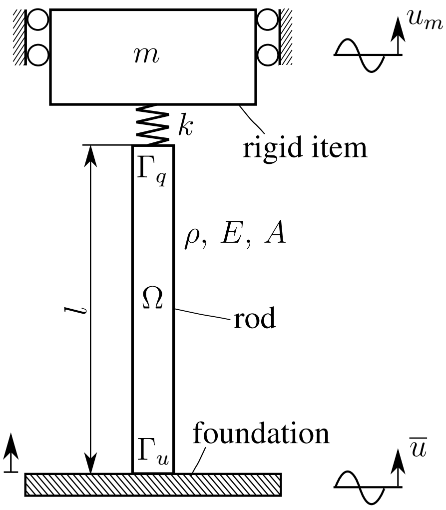

Figure 2: Schematic diagram of a rigid item mounted on an elastic rod via a spring. The excitation of the system is a displacement $\overline{u}$ of the foundation.

The rod occupies the region $\Omega = (0, l)$ in its reference state at time $t = t_0$. Its boundary $\partial\Omega$ can be decomposed into two regions $\Gamma_u \neq \emptyset$ and Γ_q, such that $\partial\Omega = \overline{\Gamma_u \cup \Gamma_q}$. The set $I = (t_0, T)$, with $T > t_0$ is a given time. Assume a displacement field $u(x,t)$ that relates the position of a material point of the rod at time t to its position at time t_0. The resulting equations of motion for waves of dilation take the form

$$\text{rod} \begin{cases} c^2 \dfrac{\partial^2 u}{\partial x^2} = \dfrac{\partial^2 u}{\partial t^2} & \text{in } \Omega \times I, \\ -EA\dfrac{\partial u}{\partial x} = k(u_m - u) & \text{on } \Gamma_q \times I, \\ u = \overline{u} & \text{on } \Gamma_u \times I, \\ u(x, t_0) = u_0(x) & \text{in } \Omega, \\ \left.\dfrac{\partial u}{\partial t}\right|_{t=t_0} = v_0(x) & \text{in } \Omega, \end{cases} \tag{1}$$

$$\text{rigid item} \begin{cases} m\dfrac{\partial^2 u_m}{\partial t^2} = -k(u_m - u) \quad \text{on } \Gamma_q \times I, \\ u_m(t_0) = u_{m,0}, \\ \left.\dfrac{\partial u_m}{\partial t}\right|_{t=t_0} = v_{m,0}, \end{cases} \tag{2}$$

where c is the propagation speed of sound and amounts to $c = \sqrt{\frac{\lambda+2\mu}{\rho}} = \sqrt{\frac{E}{\rho}}$ with λ and μ being the Lamé constants, ρ the mass density, A the rod cross-section area and E Young's modulus of the rod material. The spring element with stiffness k connects the rod with the rigid item and represents elasticities in the mount of the rigid item. The displacement of the item is described by u_m. A displacement $\overline{u}$ is prescribed on the boundary Γ_u. Also, u_0, v_0, $u_{m,0}$ and $v_{m,0}$ are the initial displacements and velocities of the rod and the rigid item, respectively.

3 WAVE-BASED ACTIVE VIBRATION ISOLATION

In this section, we present a controller for active vibration isolation which exploits wave propagation phenomena in the rod. The controller is based on the method for decomposition of traveling waves [1].

3.1 CONTROL CONCEPT

Consider the equations of motion (1) on a subset $\overline{\Omega}_d = [l_1, l_2]$ of the set $\Omega = [0, l]$, $0 \leq l_1 < l_2 \leq l$ with homogenous initial conditions in $\overline{\Omega}_d$:

$$\begin{aligned} c^2 \frac{\partial^2 u(x,t)}{\partial x^2} &= \frac{\partial^2 u(x,t)}{\partial t^2} && \text{in } \overline{\Omega}_d \times I, \\ u(x,t_0) &= 0 && \text{in } \overline{\Omega}_d, \\ \frac{\partial u(x,t_0)}{\partial t} &= 0 && \text{in } \overline{\Omega}_d. \end{aligned} \tag{3}$$

The general solution of Eq. (3) reads

$$u(x,t) = f(x - ct) + g(x + ct), \tag{4}$$

where $f(x - ct)$ represents a wave traveling in the direction of the rigid item and causing an excitation of the item. The function $g(x + ct)$ represents a wave traveling in the direction of the foundation. Knowledge of $f(x - ct)$ allows the reflection of the wave before energy can be transfered to the rigid item. Thus, an actuator can virtually modify the boundary Γ_q of the rod into a loose end. Since $f(x - ct)$ cannot be measured directly, it has to be computed from displacements u.

3.2 ALGORITHM FOR WAVE DECOMPOSITION

"Wave-based control" was introduced in series of papers, e. g. in [9], where an approximation for the calculation of traveling waves was used. In order to obtain an exact decomposition, we use a slightly modified version of the wave decomposition algorithm derived in [1]. In order to make this paper self-sufficient, the derivation of the algorithm is presented in the following.

Assume that the rod displacements $u(l_1, t) =: \Phi_1(t)$ and $u(l_2, t) =: \Phi_2(t)$ can be observed. Moreover, the parameter τ is defined such that

$$\tau := \frac{l_2 - l_1}{c} = \frac{\Delta l}{c}. \tag{5}$$

Thus, τ corresponds to the propagation time of the wave between the two observation points.

Algorithm for wave decomposition *Given the observations $\Phi_1(t)$ and $\Phi_2(t - \tau)$ as well as the past state $f(l_1 - c(t - 2\tau))$, the wave traveling in positive coordinate direction can be computed with the functional recursion $f(l_1 - ct) = \Phi_1(t) - \Phi_2(t - \tau) + f(l_1 - c(t - 2\tau))$.*

Derivation. Eq. (5) can be rewritten into

$$\begin{aligned} l_1 &= l_2 - c\tau, \\ l_2 &= l_1 + c\tau. \end{aligned} \tag{6}$$

The observations at $x = l_1$ and $x = l_2$ are

$$\begin{aligned} \Phi_1(t) &= f(l_1 - ct) + g(l_1 + ct), \\ \Phi_2(t) &= f(l_2 - ct) + g(l_2 + ct). \end{aligned} \tag{7}$$

Due to the known propagation speed c, inserting Eq. $(6)_1$ into Eq. $(7)_1$ yields

$$\Phi_1(t) = f(l_1 - ct) + g(l_2 - c\tau + ct) = f(l_1 - ct) + g(l_2 + c(t - \tau)). \tag{8}$$

Applying $(6)_2$, the observation Φ_2 at time $t - \tau$ can be written as

$$\begin{aligned} \Phi_2(t - \tau) &= f(l_2 - c(t - \tau)) + g(l_2 + c(t - \tau)) \\ &= f(l_1 + c\tau - ct + c\tau) + g(l_2 + c(t - \tau)) \\ &= f(l_1 - c(t - 2\tau)) + g(l_2 + c(t - \tau)). \end{aligned} \tag{9}$$

Hence, we arrive at

$$g(l_2 + c(t - \tau)) = \Phi_2(t - \tau) - f(l_1 - c(t - 2\tau)). \tag{10}$$

At this point, Eq. (10) is combined with Eq. (8) and solved for $f(l_1 - ct)$. Finally, we obtain the decomposed wave traveling towards the item:

$$f(l_1 - ct) = \Phi_1(t) - \Phi_2(t - \tau) + f(l_1 - c(t - 2\tau)). \tag{11}$$

3.3 AUGMENTED DYNAMICAL SYSTEM

The algorithm resulting in Eq. (11) gives rise to a novel control method for active vibration isolation. Thereby, the system described in Sec. 2 is augmented by two sensors, an actuator, a sliding carriage, and a control unit (CU). The sensors measure the displacements of two rod points. The control unit decomposes the observed displacements into traveling waves and drives the actuator. Figure 3 shows the modified system. The displacement of the sliding carriage in relation to the rod is given by $r(t) = h(t) - u_q(t)$, where $h(t)$ is the displacement of the sliding carriage in an inertial frame and $u_q(t)$ the displacement of Γ_q.

The objective of the controller is to provide a reference displacement $r^*(t)$ such that $h(t)$ vanishes. This is achieved for

$$r^*(t) = -2f\left(l_1 - c\left(t - \frac{l - l_1}{c}\right)\right) = -u_q(t). \tag{12}$$

The reference displacement $r^*(t)$ has the same amplitude but an inverted phase to the traveling wave. Furthermore, the reference displacement is shifted in time by $\frac{l - l_1}{c}$, which is exactly the time that it takes the wave to travel from the bottom sensor to the actuator.

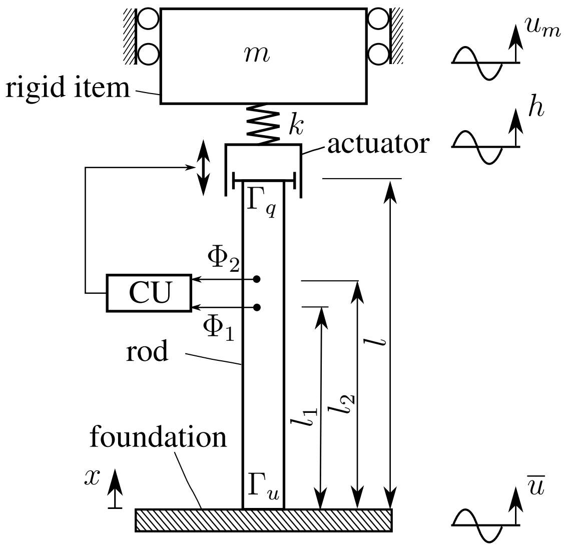

Figure 3: Schematic diagram of a wave-based active vibration isolator. The rigid item is actuated by a control unit which is processing displacement measurements of the elastic rod. The excitation of the system is a displacement $\overline{u}$ of the foundation.

4 NUMERICAL STUDIES

In this section, the controller for active vibration isolation is implemented following Sec. 3. The displacements of two rod points serve as controller inputs. A numerical example demonstrates the capabilities of the controller in an active vibration isolation context.

4.1 Discretization

In order to evaluate the controller performance in numerical studies, the equations of motion (1) have to be solved for the displacement u. Since the continuous representation lacks analytical solutions, a discretized version of Eq. (1) is derived by applying the well-known Bubnov-Galerkin method on a finite element space [10].

The domain Ω and the boundary $\partial\Omega$ are decomposed into e finite sub-domains with q nodes each. The weak form of Eq. (1) over a sub-domain Ω_e reads

$$\int_I \left[\int_{\Omega_e} \frac{\partial w^e}{\partial x} \frac{\partial u^e}{\partial x} \, \mathrm{d}\Omega_e + \int_{\Omega_e} w^e \frac{\rho}{E} \frac{\partial^2 u^e}{\partial t^2} \, \mathrm{d}\Omega_e + \int_{\partial\Omega_e} w^e \bar{t}^e \, \mathrm{d}\Gamma \right] \mathrm{d}I = 0, \tag{13}$$

where w^e is an arbitrary weighting function on $\Omega_e \times I$ and $\bar{t}^e$ is the element boundary traction satisfying

$$\bar{t}^e = \begin{cases} \frac{k}{EA}(u_m - u) \text{ in } \Gamma_q \times I & \text{if } \partial\Omega^e = \Gamma_q, \\ 0 & \text{otherwise.} \end{cases} \tag{14}$$

The exact solution u^e is approximated by a sum of polynomial shape functions $\phi^e(x)$ and the corresponding node values $u_i^e(t)$ as weights:

$$u^e \approx u_h^e = \sum_{i=1}^{q} \phi_i^e(x) u_i^e(t). \tag{15}$$

A Bubnov-Galerkin approximation is obtained by setting

$$w^e \approx w_h^e = \sum_{j=1}^{q} \phi_j^e(x)\beta_j^e(t) \tag{16}$$

with arbitrary parameters β_j^e, which are chosen to consist of Dirac-delta functions. Substitution of Eqs. (15) and (16) into Eq. (13) as well as assembling all element equations (including the equations of motion for the item (2)) yields the global system

$$\begin{aligned} \mathbf{M}\ddot{\mathbf{u}} + \mathbf{K}\mathbf{u} - \mathbf{f} &= 0 \qquad \text{in } I, \\ \mathbf{u}(t_0) &= \mathbf{u}_0, \\ \dot{\mathbf{u}}(t_0) &= \dot{\mathbf{u}}_0, \end{aligned} \tag{17}$$

where $\mathbf{u} = [\bar{u}\ \ u_2\ \ \cdots\ \ u_{e(q-1)+1}\ \ u_m]^{\mathrm{T}}$ and $\mathbf{f} = [0\ \ \cdots\ \ k(u_m - u)\ \ -k(u_m - u)]^{\mathrm{T}}$. Additionally, we introduce Rayleigh material damping. The damping matrix is assumed to be proportional to the mass and the stiffness matrix:

$$\mathbf{D} = \begin{bmatrix} \alpha\mathbf{I} & 0 \\ 0 & 0 \end{bmatrix} \mathbf{M} + \begin{bmatrix} \beta\mathbf{I} & 0 \\ 0 & 0 \end{bmatrix} \mathbf{K}, \tag{18}$$

with α and β being the damping coefficients. The system of the equations of motion can be stated as

$$\begin{aligned} \mathbf{M}\ddot{\mathbf{u}} + \mathbf{D}\dot{\mathbf{u}} + \mathbf{K}\mathbf{u} - \mathbf{f} &= 0 \qquad \text{in } I, \\ \mathbf{u}(t_0) &= \mathbf{u}_0, \\ \dot{\mathbf{u}}(t_0) &= \dot{\mathbf{u}}_0. \end{aligned} \tag{19}$$

4.2 NUMERICAL EXAMPLE

We present a numerical example for active vibration isolation via decomposition of traveling waves. Thereby, we use the system architecture described in Subsec. 3.3. The foundation is subject to a stochastic sinusoidal excitation with amplitude A_u and frequency f_u described by the stochastic differential equation

$$\mathrm{d}\bar{u} = A_u \sin(2\pi f_u t)\mathrm{d}t + \sigma \mathrm{d}W(t). \tag{20}$$

Here, $W(t)$ represents a standard Wiener process and σ is the standard deviation. Two sensors at $x = l_1$ and $x = l_2$ observe the axial displacements. The decomposition algorithm provides the reference displacement $r^*(t)$. For simplicity, we assume that the sliding carriage is able to follow r^* exactly. The Newmark-beta method with time step size Δt is chosen for time integration of Eq. (19). Table 1 lists an overview of the system and simulation parameters.

Table 1: System and simulation parameters.

Parameter	Value	Parameter	Value
Rod length l:	1 m	Excitation frequency f_u:	5 Hz
Propagation speed c:	1600 m/s	Time step size Δt:	10^{-6} s
Rigid item mass m:	0.03 kg	Damping coefficient α:	$5 \cdot 10^{-6}$
Spring constant k:	200 kN/mm	Damping coefficient β:	$5 \cdot 10^{-6}$
First sensor position l_1:	0.70 m	Finite elements e:	100
Second sensor position l_2:	0.74 m	Element nodes q:	2

The results of a numerical realization are displayed in Fig. 4. The foundation excitation is plotted as a black line. The dashed blue line represents the response of the item without the influence of the controller. The red vertical line at $t = 1\,\mathrm{s}$ marks the time when the control algorithm is turned on. The continuous blue line shows the displacement of the item under the influence of the control algorithm. It is clearly visible from Fig. 4 that the vibrations of the item are instantly cured, because almost all of the vibration energy is reflected by the actuator before it can influence the item.

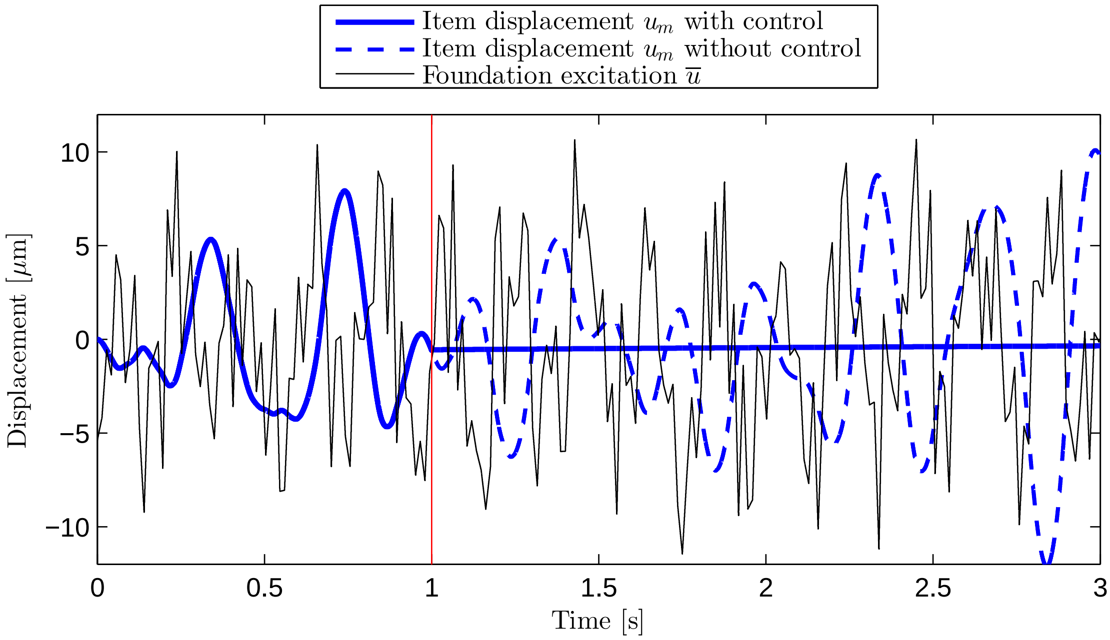

Figure 4: Comparison of the item displacement without controller (blue, dashed curve) and with controller turned on at 1 s (blue, continuous curve). The black curve refers to the foundation excitation.

5 EXPERIMENTAL RESULTS FOR MEASURING WAVE EFFECTS

The goal of the experimental setup is to demonstrate that the delicate measurements required as inputs into the control algorithm derived in Sec. 3 can be realized with currently available technology. Thereby, the crucial measurement requirements are the capturing of the small amplitudes of axial displacements and the correct resolution on the time scale. While the small amplitudes could already be measured in [11], we want to show that the propogation time of the axial wave between two distinct measurement points leads to a delay in the corresponding measurement signals.

The setup used for experimental investigations is shown schematically in Fig. 5a. A brass rod of length $l = 1.2\,\mathrm{m}$ is fixed to a rigid mounting with zero displacement. A force is applied to the bottom of the rod resulting in an axial wave traveling upwards the rod. The axial displacements of the rod are measured using two laser displacement sensors of type optoNCDT 2300-2 made by Micro-Epsilon Messtechnik GmbH & Co. KG. Thereby, two ceramic wedges are fixed on the rod and reflect the laser beams, see Fig. 5b. The displacements are computed via triangulation. Sensor 1 is placed at $l_1 = 0.08\,\mathrm{m}$ and sensor 2 at $l_2 = 0.58\,\mathrm{m}$. The sampling frequency of the sensors is $f_s = 48.9\,\mathrm{kHz}$.

Given a propagation speed of $c_{\text{brass}} = 3530\,\mathrm{m/s}$, the expected number of samples between the response of sensor 1 and sensor 2 amounts to seven. That is the amount of samples which is

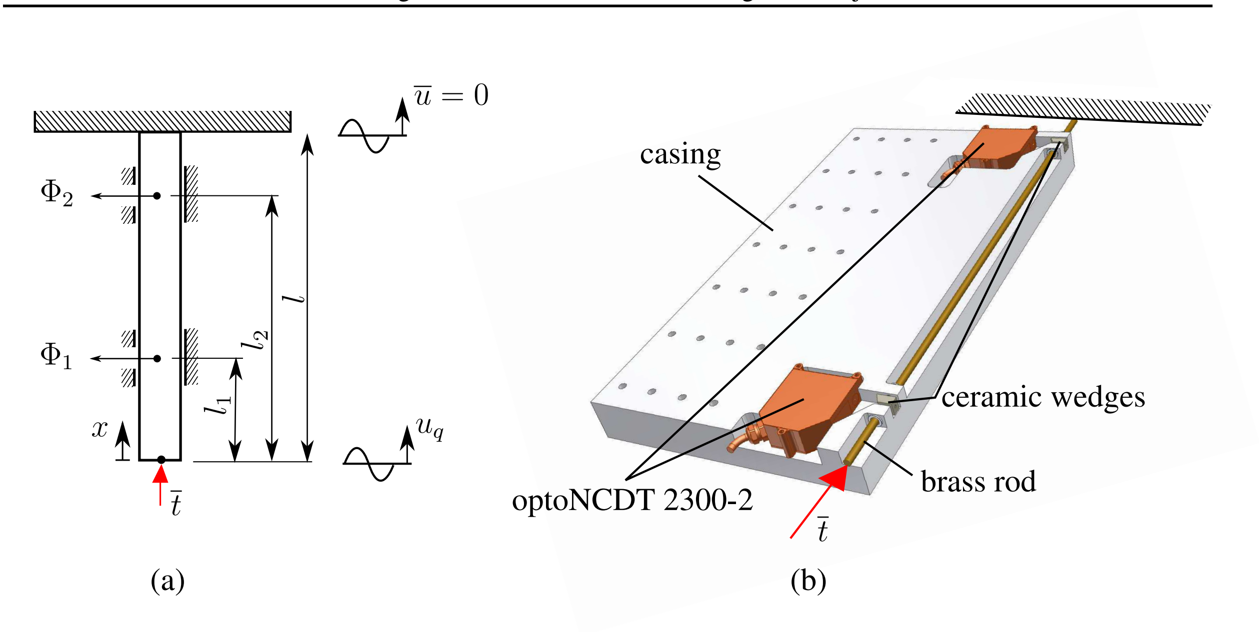

Figure 5: Experimental setup for measuring wave effects in an elastic rod: (a) Schematic representation. (b) CAD drawing.

expected for the wave to travel from sensor 1 to sensor 2. The time evolution of the impact force as well as the measured axial displacements Φ_1 and Φ_2 are presented in Fig. 6. The time delay in the experiment is in a good agreement with the calculated seven samples. This demonstrates the feasibility of the measurements required for the decomposition into traveling waves.

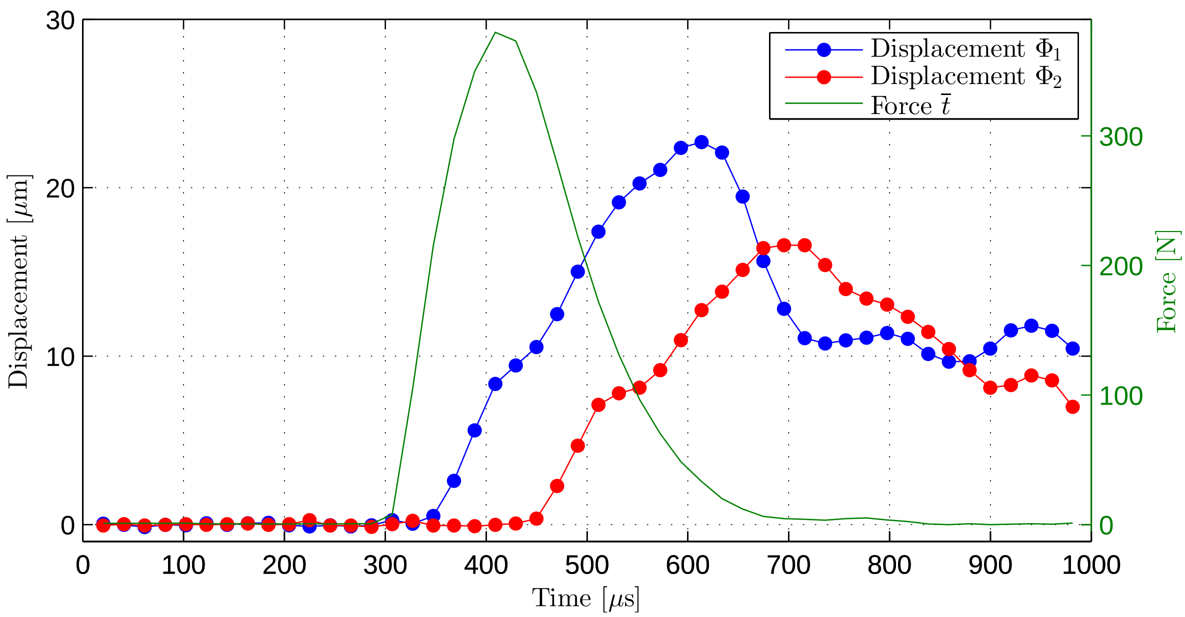

Figure 6: Measured displacement responses Φ_1 (blue curve) and Φ_2 (red curve) to the impact force $\bar{t}$ (green curve).

6 CONCLUSION

In this paper, we present a novel approach for active vibration isolation. We consider a group of systems with distributed isolator mass, for which wave effects occur. As an example, a system is examined consisting of a rigid item fixed to an elastic rod which is subject to foundation excitations. Waves traveling in the direction of the rigid item are responsible for its excitation. We propose a control law that decomposes axial displacements of the rod into two waves of opposite propogation directions. With this control law, only two sensors are required and can be placed arbitrarily along the rod as long as no forces act in between. Additionally, only the speed of sound of the rod material has to be known for controller synthesis. Using the decomposition results, a linear actuator can reflect the undesired waves traveling towards the item, thus hindering energy propogation to the item. The reflection coefficient of the actuator can be realized to one over a wide band of frequencies. Performance of the proposed control algorithm is shown for a numerical example. Despite the stochastic foundation excitation, the item is isolated very effectively. Furthermore, we demonstrate with an experimental setup that the necessary measurements can be realized with the required precision. This is the groundwork for a future hardware implementation of the presented vibration isolation concept.

REFERENCES

[1] Kreuzer, E. ; Steidl, M.: Controlling torsional vibrations of drill strings via decomposition of traveling waves. *Archive of Applied Mechanics* **82**(4), 515-531, 2012.

[2] Crede, C.E. ; Ruzicka, J.E.: Theory of Vibration Isolation, In: Harris, C.M. ; Piersol, A.G. (Eds.): *Harris'Shock and Vibration Handbook*. McGraw-Hill Professional, New York, NY, 30-1 - 30-57, 2002.

[3] Ibrahim, R.A.: Recent advances in nonlinear passive vibration isolators. *Journal of Sound and Vibration* **314**(3-5), 371-452, 2008.

[4] Rakheja, S. ; Sankar, S.: Vibration and Shock Isolation Performance of a Semi-Active "On-Off" Damper. *Journal of Vibration and Acoustics* **107**(4), 398-403, 1985.

[5] Liu, Y. ; Waters, T.P. ; Brennan, M.J.: A comparison of semi-active damping control strategies for vibration isolation of harmonic disturbances. *Journal of Sound and Vibration* **280**(1-2), 21-39, 2005.

[6] Yan, B. ; Brennan, M.J. ; Elliott, S.J. ; Ferguson, N.S.: Active vibration isolation of a system with a distributed parameter isolator using absolute velocity feedback control. *Journal of Sound and Vibration* **329**(10), 1601-1614, 2010.

[7] Collette, C ; Janssens, S. ; Artoos, K.: Review of Active Vibration Isolation Strategies. *Recent Patents on Mechanical Engineering* **4**(3), 1-8, 2011.

[8] Timoshenko, S.P. ; Goodier, J.N.: *Theory of Elasticity*. McGraw-Hill Kogakusha, New York, NY, 1987.

[9] O'Connor, W.J.: Wave-based analysis and control of lump-modeled flexible robots. *IEEE Transactions on Robotics* **24**(2), 342-352, 2007.

[10] Zienkiewicz, O.C. ; Taylor, R.L.: *The Finite Element Method: Its Basis and Fundamentals*. Butterworth-Heinemann, Oxford, UK, 2005.

[11] Seifried, R. ; Eberhard, P.: Comparison of numerical and experimental results for impacts. *Proceedings of the ENOC*, 399-408, 2005.